Sensitivity of an Ocean-Atmosphere Coupled Model to the Coupling Method : Example of Tropical Cyclone Erica

Florian Lemarié, Patrick Marchesiello, Laurent Debreu, Eric Blayo

Sensitivity of an Ocean-Atmosphere Coupled Model to the Coupling Method : Study of Tropical Cyclone Erica

Florian Lemarié [a,*] , Patrick Marchesiello [b], Laurent Debreu [a], Eric Blayo [c,a]

[a] *INRIA Grenoble Rhône-Alpes and Jean Kuntzmann Laboratory, 38000 Grenoble, France*

[b] *LEGOS, IRD, 14, Avenue Edouard Belin, 31400 Toulouse, France*

[c] *Université Grenoble-Alpes, 38000 Grenoble, France*

Abstract

In this paper, the sensitivity of Atmospheric and Oceanic Coupled Models (AOCMs) to the associated coupling method is investigated. We propose the adaptation of a Schwarz-like domain decomposition method to AOCMs. We show that this kind of iterative process ensures a good consistency of the coupled solution across the air-sea interface, while usual *ad-hoc* algorithmic approaches do not properly satisfy this requirement. Indeed, those *ad-hoc* methods correspond to only one iteration of a Schwarz-like iterative method, without reaching a converged state. Until now, it was assumed that this lack of consistency does not affect significantly the physical properties of the solution. The relevancy of this statement is assessed in the context of a coupling between a mesoscale atmospheric model (WRF) and a regional oceanic model (ROMS) in a realistic configuration aiming at simulating the genesis and propagation of tropical cyclone Erica. Sensitivity tests to the coupling method are carried out in an ensemblist approach. We show that with a mathematically consistent coupling the spread of the ensemble is reduced, thus suggesting that there is room for further improvements in the formulation of AOCMs at a mathematical and numerical level.

1 Introduction

1.1 Context

Many applications in global/regional oceanography and meteorology require Atmospheric and Oceanic Coupled Models (AOCMs) which account for important air-sea feedbacks. Separate integrations of the

* Corresponding author.
Phone: +33 (0)4 76 51 48 60
Fax: +33 (0)4 76 63 12 63
E-mail address: florian.lemarie@inria.fr .

oceanic and atmospheric numerical models in a forced mode (i.e. without retroaction from one component to the other) may be satisfactory for numerous applications and process studies (e.g. Marchesiello et al., 2003; Colas et al., 2011; Lemarié et al., 2012). However, two-way coupling is essential for analyzing energetic and complex phenomena like tropical cyclones, eastern boundary upwellings (e.g. Bao et al., 2000; Perlin et al., 2007; Capet et al., 2008), and more generally climate trends (e.g. Large and Danabasoglu, 2006; Terray et al., 2011). In this case, connecting the two model solutions at the air-sea interface is an arduous task which jointly raises mathematical, physical and computational issues.

Besides the numerical models of the ocean and the atmosphere, the formulation of AOCMs is based on several components : a parameterization of the turbulent air-sea fluxes, a coupling infrastructure, and a coupling algorithm. Several parameterizations of the evolution of the atmospheric flow in the surface layer under the influence of the oceanic surface have been designed. Those parameterizations are derived at a semi-empirical level and are based on field and laboratory experiments designed to carefully tune number of parameter values (Fairall et al., 2003; Large, 2006). As far as the computational issues are concerned, numerous coupling softwares have been developed over the last ten years (Hill et al., 2004; Joppich and Kürschner, 2006; Redler et al., 2010). Those tools are necessary to handle the message passing, the synchronization in time and the regridding procedure (i.e. interpolation/extrapolation) between the computational grids of the models under consideration. The last ingredient, of numerical nature, in the design of an AOCM is a *consistent* coupling algorithm; this is the main subject of this paper. The notion of *consistency* associated with the ocean atmosphere coupling problem will be clarified below in Sec. 1.2.

It is known that AOCMs solutions exhibit a strong sensitivity to model parameters (Bengtsson, 1999; McWilliams, 2007). More specifically, sensitivity to perturbations in the initial conditions (Ploshay and Anderson, 2002), to the coupling frequency (Lebeaupin Brossier et al., 2009; Terray et al., 2011; Masson et al., 2012), and to the air-sea fluxes formulation (Lebeaupin Brossier et al., 2008) have been observed, on top of the internal sensitivities in the numerical models themselves (Tribbia and Baumhefner, 1988). This is arguably a source of concern when it comes to assess the degree of plausibility of the AOCMs solution. Uncertainties in the specification of the air-sea fluxes is strongly related to the empirical nature of the atmospheric surface layer parameterizations resulting from the extreme complexity of the processes to represent. In general, a given parameterization is designed and tuned for a particular geographical region or for a particular range of static stability. A lot of efforts are being directed toward improving physical parameterizations because these are usually considered as the major errors in AOCMs. However, we argue that it is also crucial to keep working on other model developments to identify other possible sources of error/deficiency. Preliminary studies of the fifth phase of the Coupled Model Comparison Project (CMIP5) do not report significant improvements in biases in present-day climate compared to CMIP3 (e.g. Roehrig et al., 2013; Sen Gupta et al., 2013). This suggests that finer horizontal resolution is not sufficient to cure the aforementioned problems. There is clearly a need for a more complete understanding of what goes on in numerical coupled models, notably through a finer consideration of numerical methods and modelling assumptions. To our knowledge, no systematic sensitivity study to the algorithmic aspects of air-sea coupling has been carried out so far. We investigate this sensitivity in the present paper, starting with the definition of the coupled problem under investigation.

1.2 Coupling Problem

We symbolically describe the oceanic and atmospheric circulation models by partial differential operators $\mathcal{L}_{\mathrm{oce}}$ and $\mathcal{L}_{\mathrm{atm}}$ corresponding to the systems of equations solved by numerical models. Traditionally,

we consider the primitive equations in the ocean and the fully-compressible Euler equations in the atmosphere. On the computational domain $\Omega = \Omega_{\rm atm} \cup \Omega_{\rm oce}$ (with external boundaries $\partial\Omega^{\rm ext}_{\rm atm}$ and $\partial\Omega^{\rm ext}_{\rm oce}$, see Fig. 1), the integration over a time period $[0, \mathcal{T}]$ corresponds to

$$\begin{cases} \mathcal{L}_{\rm atm}\mathbf{U}^{\rm a} = f_{\rm atm}, & \text{in } \Omega_{\rm atm} \times [0, \mathcal{T}], \\ \mathcal{B}_{\rm atm}\mathbf{U}^{\rm a} = g_{\rm atm}, & \text{in } \partial\Omega^{\rm ext}_{\rm atm} \times [0, \mathcal{T}], \\ \mathcal{F}_{\rm atm}\mathbf{U}^{\rm a} = \mathbf{F}_{\rm oa}(\mathbf{U}^{\rm o}, \mathbf{U}^{\rm a}, \mathcal{R}), & \text{on } \Gamma \times [0, \mathcal{T}], \end{cases} \tag{1.1}$$

$$\begin{cases} \mathcal{L}_{\rm oce}\mathbf{U}^{\rm o} = f_{\rm oce}, & \text{in } \Omega_{\rm oce} \times [0, \mathcal{T}], \\ \mathcal{B}_{\rm oce}\mathbf{U}^{\rm o} = g_{\rm oce}, & \text{in } \partial\Omega^{\rm ext}_{\rm oce} \times [0, \mathcal{T}], \\ \mathcal{F}_{\rm oce}\mathbf{U}^{\rm o} = \mathbf{F}_{\rm oa}(\mathbf{U}^{\rm o}, \mathbf{U}^{\rm a}, \mathcal{R}), & \text{on } \Gamma \times [0, \mathcal{T}], \end{cases} \tag{1.2}$$

with appropriate boundary conditions provided through the boundary operators $\mathcal{B}_{\rm oce}$ and $\mathcal{B}_{\rm atm}$ (the initialization of coupled models is an open problem that is beyond the scope here). In (1.1) and (1.2), $\mathbf{U}^{\rm a} = (\mathbf{u}^{\rm a}_h, T^{\rm a})^t$ and $\mathbf{U}^{\rm o} = (\mathbf{u}^{\rm o}_h, T^{\rm o})^t$ are the state variables with $\mathbf{u}_h$ the horizontal velocity and T the (potential) temperature, $f_{\rm atm}$ and $f_{\rm oce}$ are forcing terms. For the sake of simplicity, we focus on temperature and momentum, we do not include salinity and humidity in the continuous formulation of the problem (it is however included in the practical application discussed in Sec. 5). The oceanic domain $\Omega_{\rm oce}$ and the atmospheric domain $\Omega_{\rm atm}$ have a common interface Γ (Fig. 1). $\mathbf{F}_{\rm oa}$ is a function allowing the computation of air-sea fluxes. This function, generally based on the atmospheric surface layer similarity theory (e.g. Large, 2006), depends on $\mathbf{U}^{\rm a}$ and $\mathbf{U}^{\rm o}$ in the vicinity of the air-sea interface (as shown in Fig. 1), and on a set of non-turbulent radiative fluxes $\mathcal{R}$.

In (1.1)-(1.2), the interface operators are defined as

$$\mathcal{F}_{\rm atm}\bullet = \rho^{\rm a}\mathbf{K}^{\rm a}\partial_z\bullet, \qquad \mathcal{F}_{\rm oce}\bullet = \rho^{\rm o}\mathbf{K}^{\rm o}\partial_z\bullet,$$

where z is positive upward, $\rho^{\rm a}$ and $\rho^{\rm o}$ are the densities of the fluids, and

$$\mathbf{K}^{\rm a} = \begin{pmatrix} \mathrm{K}^{\rm a}_{\rm m} \\ \mathrm{K}^{\rm a}_{\rm m} \\ c^{\rm a}_p\mathrm{K}^{\rm a}_{\rm t} \end{pmatrix}, \qquad \mathbf{K}^{\rm o} = \begin{pmatrix} \mathrm{K}^{\rm o}_{\rm m} \\ \mathrm{K}^{\rm o}_{\rm m} \\ c^{\rm o}_p\mathrm{K}^{\rm o}_{\rm t} \end{pmatrix}.$$

We note $\mathrm{K}^{\rm a}_{\rm m}$ and $\mathrm{K}^{\rm o}_{\rm m}$ the eddy viscosities, and $\mathrm{K}^{\rm a}_{\rm t}$ and $\mathrm{K}^{\rm o}_{\rm t}$ the eddy diffusivities. The c_p terms correspond to the specific heat of the fluid.

In a forced mode, $\mathbf{U}^{\rm o}$ (resp. $\mathbf{U}^{\rm a}$ and $\mathcal{R}$) in (1.1) (resp. (1.2)) is provided offline by existing satellite-based or reanalysis-based products. In a coupled mode, both models are run either simultaneously or successively on the same space-time interval. In this case, the consistency required at the air-sea interface is the continuity of the vertical fluxes

$$\begin{aligned} \rho^{\rm a}\mathrm{K}^{\rm a}_{\rm m}\partial_z\mathbf{u}^{\rm a}_h = \rho^{\rm o}\mathrm{K}^{\rm o}_{\rm m}\partial_z\mathbf{u}^{\rm o}_h \ &= \boldsymbol{\tau} && \text{on } \Gamma \times [0, \mathcal{T}] \\ \rho^{\rm a}c^{\rm a}_p\mathrm{K}^{\rm a}_{\rm t}\partial_z T^{\rm a} = \rho^{\rm o}c^{\rm o}_p\mathrm{K}^{\rm o}_{\rm t}\partial_z T^{\rm o} &= Q_{\rm net} = \mathcal{R} + Q_{\rm S} && \text{on } \Gamma \times [0, \mathcal{T}] \end{aligned}$$

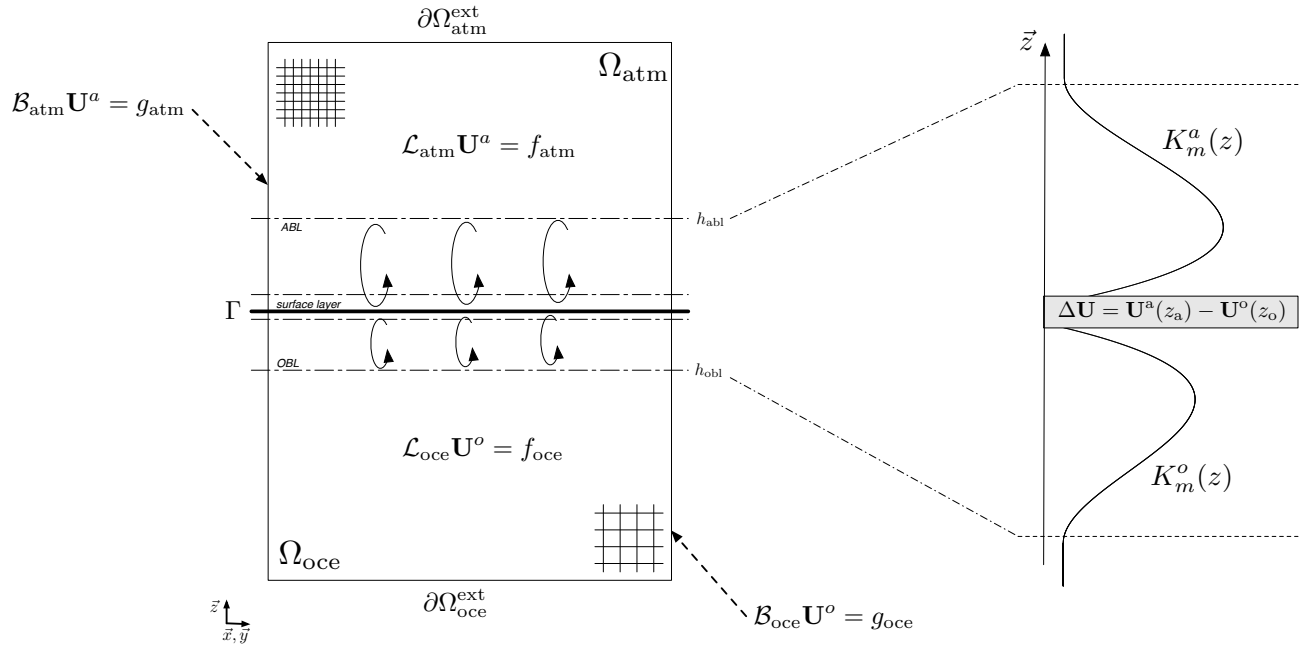

Fig. 1. Schematic view of the two non-overlapping subdomains $\Omega_{\rm atm}$ and $\Omega_{\rm oce}$. The mathematical notations correspond to those introduced in Sec. 1.2. The boundary layers encompassing the air-sea interface Γ and the atmospheric surface layer (gray shaded) are of particular importance for the coupling problem. The quantity $\Delta\mathrm{U} = \mathbf{U}^{\rm a}(z_{\rm a}) - \mathbf{U}^{\rm o}(z_{\rm o})$ is directly involved in the computation of air-sea fluxes, with z_a (resp. z_o) the location of the lowest (resp. shallowest) vertical level in the atmospheric (resp. oceanic) model.

where the surface wind stress $\boldsymbol{\tau}$ and the sensible heat flux $Q_{\rm S}$ (consequently the net heat flux $Q_{\rm net}$) are computed using the function $\mathbf{F}_{\rm oa} = (\boldsymbol{\tau}, Q_{\rm net})^t$ previously introduced. Those turbulent air-sea fluxes are given by a parameterization of the atmospheric surface layer. They usually take the form

$$\boldsymbol{\tau} = \rho^{\rm a} C_D \|\Delta\mathrm{U}\| \Delta\mathrm{U}, \qquad Q_{\rm S} = \rho^{\rm a} c_p^{\rm a} C_H \|\Delta\mathrm{U}\| \Delta T, \tag{1.3}$$

where C_D and C_H are exchange coefficients which generally depend on the local stratification. ΔU (resp. ΔT) correspond to the velocity (resp. temperature) jump across the air-sea interface which is defined, in a bulk way, as the region between the lowest vertical level in the atmospheric model and the shallowest vertical level in the oceanic model.

At this point we have defined all the necessary notations to formulate the coupled problem under interest throughout this paper :

Find $\mathbf{U}^{\rm a}$ and $\mathbf{U}^{\rm o}$ that satisfy

$$\begin{cases} \mathcal{L}_{\rm atm}\mathbf{U}^{\rm a} = f_{\rm atm} & \text{in } \Omega_{\rm atm} \times [0, \mathcal{T}] \\ \mathcal{B}_{\rm atm}\mathbf{U}^{\rm a} = g_{\rm atm} & \text{in } \partial\Omega^{\rm ext}_{\rm atm} \times [0, \mathcal{T}] \\ \mathcal{L}_{\rm oce}\mathbf{U}^{\rm o} = f_{\rm oce} & \text{in } \Omega_{\rm oce} \times [0, \mathcal{T}] \\ \mathcal{B}_{\rm oce}\mathbf{U}^{\rm o} = g_{\rm oce} & \text{in } \partial\Omega^{\rm ext}_{\rm oce} \times [0, \mathcal{T}] \\ \mathcal{F}_{\rm atm}\mathbf{U}^{\rm a} = \mathcal{F}_{\rm oce}\mathbf{U}^{\rm o} = \mathbf{F}_{\rm oa}(\mathbf{U}^{\rm o}, \mathbf{U}^{\rm a}, \mathcal{R}) & \text{on } \Gamma \times [0, \mathcal{T}] \end{cases} \tag{1.4}$$

for given initial and boundary conditions. It is worth mentioning that Lions et al. (1995) proved the exis-

tence of a global weak solution to problem (1.4) with interface conditions given by (1.3), considering that $\mathcal{L}_{\mathrm{atm}}$ and $\mathcal{L}_{\mathrm{oce}}$ are the primitive equations of the atmosphere and the ocean.

This paper is organized as follows. The existing coupling methods currently in use to solve (1.4) are presented in Sec. 2. In Sec. 3, we provide critical comments about those methods and we introduce a new theoretical framework to pose the coupling problem. In Sec. 4 we present the formulation of our AOCM based on the Weather Research and Forecasting (WRF, Skamarock and Klemp, 2008) model and the Regional Oceanic Modeling System (ROMS, Shchepetkin and McWilliams, 2005). In Sec. 5 we assess the sensitivity of this model to the algorithmic approach for the simulation of a tropical cyclone. We show that a mathematically consistent algorithmic approach leads to less sensitivity of the coupled solution to perturbations in the initial condition and coupling frequency. We summarize and discuss our findings in Sec. 6.

2 A Classification of Existing Methods

Coupling methods can be categorized in two different groups : 1-way algorithms, when one model receive informations but does not send anything back to the other, and 2-way algorithms, when a feedback is introduced. The 1-way strategies (e.g. Muller et al., 2007) are beyond the scope here, we focus on the 2-way algorithms. The usual coupling strategies can be found in Bryan et al. (1996) mostly for global configurations and in Bao et al. (2000) and Perlin et al. (2007) mostly for regional high-resolution studies. A first algorithmic approach generally used for global problems is based on the exchange of averaged-in-time fluxes between the models (usually referred to as *asynchronous* coupling) whereas a second one deals with instantaneous fluxes (usually referred to as *synchronous* coupling). In this section, we expose the key differences between both strategies.

2.1 Asynchronous Coupling by Time Windows (Based on Mean Fluxes)

The asynchronous coupling is the strategy used by most of the IPCC [1] -like climate models. For this method, the total simulation time $[0, \mathcal{T}]$ is split into M smallest time windows $[t_i, t_{i+1}]$, i.e. $[0, \mathcal{T}] = \cup_{i=1}^{M} [t_i, t_{i+1}]$. The length of those time windows can be typically between 1 hour and 1 day depending on the target applications and the need to resolve or not the diurnal cycle. On a given time window, the atmospheric and the oceanic models exchange only averaged-in-time quantities. This approach has the advantage to require few communications between the models. By noting $\langle . \rangle_i$ a temporal average on the time window $[t_i, t_{i+1}]$, the coupling strategy can be described by

$$\left\{ \begin{array}{ll} \mathcal{L}_{\rm atm} \mathbf{U}^{\rm a} = f_{\rm atm} & \text{in } \Omega_{\rm atm} \times [t_i, t_{i+1}] \\ \mathcal{F}_{\rm atm} \mathbf{U}^{\rm a} = \mathbf{F}_{\rm oa}(\langle \mathbf{U}^{\rm o} \rangle_{i-1}, \mathbf{U}^{\rm a}, \mathcal{R}) & \text{on } \Gamma \times [t_i, t_{i+1}] \end{array} \right.$$
$$\text{then} \qquad (2.1)$$
$$\left\{ \begin{array}{ll} \mathcal{L}_{\rm oce} \mathbf{U}^{\rm o} = f_{\rm oce} & \text{in } \Omega_{\rm oce} \times [t_i, t_{i+1}] \\ \mathcal{F}_{\rm oce} \mathbf{U}^{\rm o} = \langle \mathcal{F}_{\rm atm} \mathbf{U}^{\rm a} \rangle_i & \text{on } \Gamma \times [t_i, t_{i+1}] \end{array} \right.$$

This algorithm is schematically described in Fig. 2. First the atmospheric model is advanced from t_i to t_{i+1} using the averaged ocean state computed on the previous time window. Then, the fluxes used to force the atmospheric model are averaged and applied to the oceanic model on the same time interval (the fluxes are generally piecewise constant on each time window). This methodology ensures that over a time interval $[t_i, t_{i+1}]$ both models are forced by the exact same mean fluxes, which ensures a strict conservation of the quantities. Indeed, in both models the integral of the surface fluxes will be equal to $\langle \mathcal{F}_{\rm atm} \mathbf{U}^{\rm a} \rangle_{[0,\mathcal{T}]}$.

The solution of algorithm (2.1) is however not rigorously solution of the original problem (1.4) because both models are not in exact balance on the time interval $[t_i, t_{i+1}]$. The modification of the oceanic state $\mathbf{U}^{\rm o}$ is not "felt" by the atmospheric component on the proper time interval $[t_i, t_{i+1}]$ but only on $[t_{i+1}, t_{i+2}]$. It is usually assumed that this lack of synchronization does not impair significantly the coupled solution, even if this algorithmic approach leads to some significant numerical errors, as discussed in Sec. 3.2.

[1] Intergovernmental Panel on Climate Change

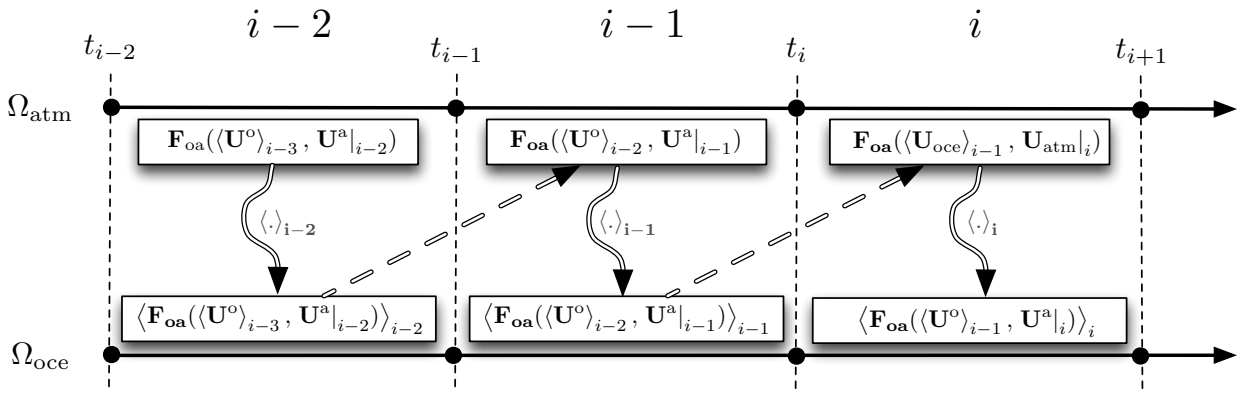

Fig. 2. Schematic view of the coupling by time windows. Three time windows, numbered from $i-2$ to i, are considered here. The arrows correspond to an exchange of information between both models. The operator $\langle . \rangle_i$ denotes a temporal average over the time window i.

2.2 Synchronous Coupling at the Time Step Level (Based on Instantaneous Fluxes)

In nature, the ocean and the atmosphere continuously exchange fluxes on scales ranging from global to micro scales. Hence, we could consider that a proper coupling frequency between the numerical models should be as small as possible, typically the largest time step between the oceanic and the atmospheric model. In this regard, a relevant algorithm would consist in exchanging instantaneous fluxes. Let us consider that the oceanic time step Δt_o is such that $\Delta t_o = N \Delta t_a$. The corresponding algorithm reads

$$\left\{ \begin{array}{ll} \mathcal{L}_{\rm atm} \mathbf{U}^{\rm a} = f_{\rm atm} & \text{in } \Omega_{\rm atm} \times [t_i, t_i + N\Delta t_a] \\ \mathcal{F}_{\rm atm} \mathbf{U}^{\rm a} = \mathbf{F}_{\rm oa}(\mathbf{U}^{\rm o}(t_i), \mathbf{U}^{\rm a}(t), \mathcal{R}(t)) & \text{on } \Gamma \times [t_i, t_i + N\Delta t_a] \end{array} \right. \tag{2.2}$$

$$\left\{ \begin{array}{ll} \mathcal{L}_{\rm oce} \mathbf{U}^{\rm o} = f_{\rm oce} & \text{in } \Omega_{\rm oce} \times [t_i, t_i + \Delta t_o] \\ \mathcal{F}_{\rm oce} \mathbf{U}^{\rm o} = \mathbf{F}_{\rm oa}(\mathbf{U}^{\rm o}(t_i), \mathbf{U}^{\rm a}(t_i), \mathcal{R}(t_i)) & \text{on } \Gamma \times [t_i, t_i + \Delta t_o] \end{array} \right.$$

Typically, the oceanic and atmospheric components are integrated forward for a time period corresponding to Δt_o (or equivalently $N \Delta t_a$). Data exchange of instantaneous values is then performed and model integration continues for an other Δt_o period of time. This process is repeated until the final forecast time (Fig. 3). In (2.2) the oceanic component receives instantaneous values from the atmosphere but we also could have considered integrated values between t_i and $t_i + N\Delta t_a$ to avoid aliasing errors (Fig. 3,b), but both approaches raise conservation or synchronisation problems. Algorithm (2.2) is difficult to implement efficiently from the numerical and computational point of view. Indeed, the communications between both codes are extremely frequent and the time integration schemes under consideration must be carefully studied to get a consistent exchange of boundary conditions.

At first glance, we could think that (2.2) is solution of the full problem (1.4). This is, however, formally true only for $\Delta t_o, \Delta t_a \to 0$. In most numerical models, the vertical diffusion is treated implicitly-in-time the air-sea fluxes are thus expected to be provided at time $t_i + \Delta t$ and not at time t_i as in (2.2). As for algorithm (2.1), it can be shown that this inaccuracy in the specification of the boundary conditions leads to an erroneous method (Sec. 3.2).

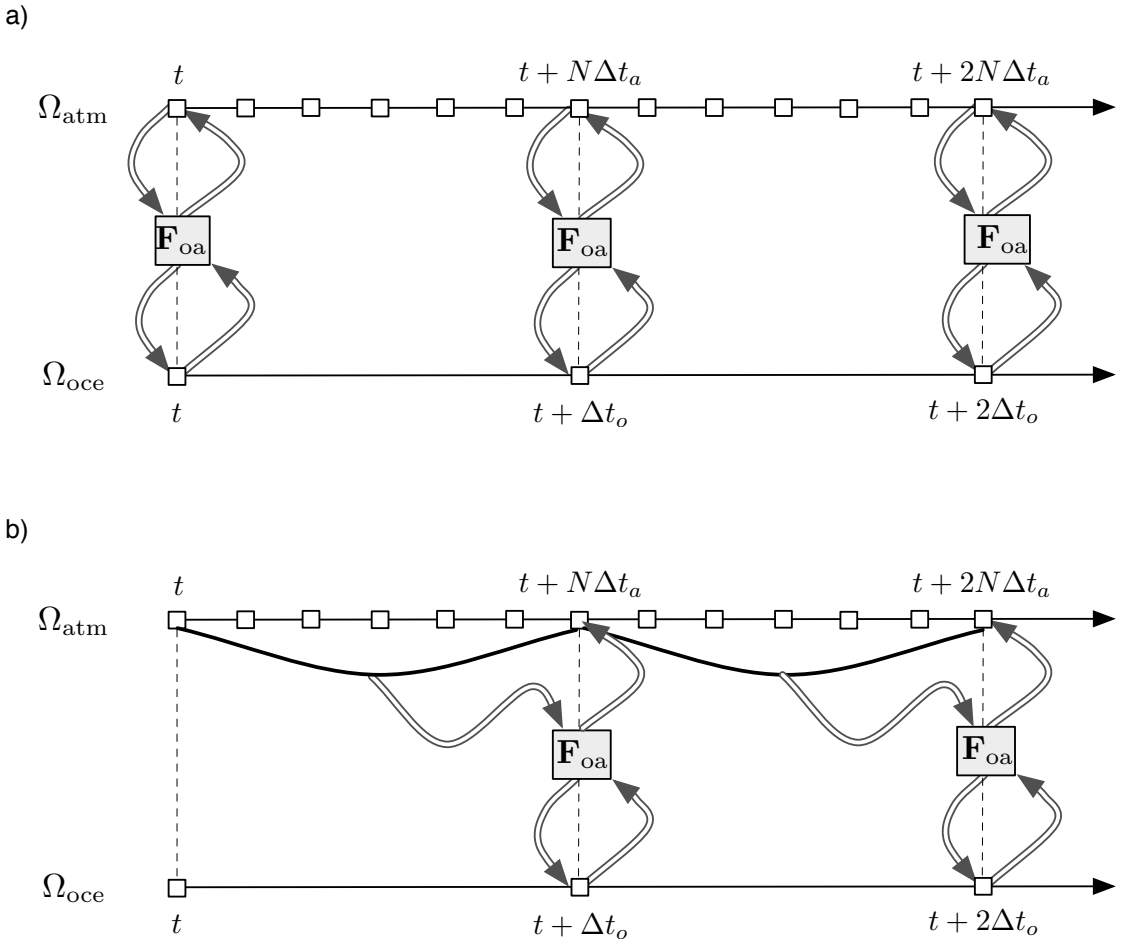

Fig. 3. Example of two coupling strategies at the time step level. Δt_o and Δt_a denote the (baroclinic) time steps respectively of the oceanic and the atmospheric models, with $\Delta t_o = N\Delta t_a$ ($N = 6$ here). The arrows represent an exchange of information with the surface layer parameterization function $\mathbf{F}_{\mathrm{oa}}$. For the atmospheric component this exchange is based on instantaneous values for algorithm a) and on integrated in time values for algorithm b).

3 Numerical and Physical Considerations

In the previous section, we showed that the numerical methods generally used to solve the coupled problem (1.4) are not fully satisfying from a mathematical point of view. In this section, we first discuss the specificities of the ocean-atmosphere coupling problem and we then propose an alternative method to solve it.

3.1 Specificities of the Ocean-Atmosphere Coupling

Coupling methods used in the context of AOCMs differ from the methods usually used for multi-physics (fluid-fluid) coupling. However, the latter can not be easily applied to AOCMs because they often assume a full representation of all the spatio-temporal scales involved in the problem. The oceanic and

atmospheric variability is spectrally broad band across all scales from micro $\mathcal{O}(10^{-3}\text{ m}, 10^{-3}\text{ s})$ to global $\mathcal{O}(10^{7}\text{ m}, 10^{10}\text{ s})$ scales. AOCMs contain essential parameterization to account for unresolved processes. The fluxes exchanged by the models are not the result of a discrete derivative in the vicinity of the air-sea interface but are given by atmospheric surface layer parameterizations based on the so-called bulk aerodynamic method, which are symbolically represented by the function F_{oa} in (1.4). Those parameterizations are defined and calibrated semi-empirically using measurements averaged in time over about an hour or more, and for a restricted range of stability values. There is a lack of accurate knowledge and observations of air-sea fluxes at high temporal scales (see discussion in Danabasoglu et al. (2006), Sec. 2). The sign of air-sea fluxes is uncertain on time scales less than 10 minutes and hourly fluxes are more relevant (Large, 2006). Indeed, the bulk formulations generally neglect the physical processes relevant to high frequency coupling, such as spray contributions to heat fluxes and the wavy boundary layer (Bao et al., 2000). For problems involving physical parameterizations, an additional time scale is imposed by the physics to be valid. This *physical time step* is generally different from the dynamical time step of the numerical models. The error associated with the $\mathbf{F}_{\mathrm{oa}}$ function increases significantly when the averaging time decreases (see discussion in Sec. 7 in Large (2006)). This growing error of parameterization is further added to the intrinsic errors related to the coupling scheme. That is why an averaging in time, acting as a smoother to remove smallest time scales, is preferable and is adopted in algorithm (2.1). Hence, we can consider that algorithm (2.2) is relevant only if additional physical processes predominant on short time-scales are explicitly taken into account in the flux computation, which is still a work very much in its infancy, and requires a careful consideration of the assumptions behind the Bulk formulae.

3.2 Numerical Considerations

We showed in Sec. 2 that the usual numerical methods used in AOCMs are not entirely satisfactory from a numerical viewpoint. To make thinks easier to understand, we define a simplified one-dimensional coupling problem with an interface at $z = 0$:

$$\begin{cases} \partial_t q_2 - \partial_z(\nu_2 \partial_z q_2) = f_2, & \text{in }]0, L_2[\times[0,\mathcal{T}], \\ q_2(L_2, t) = 0, & t \in [0,\mathcal{T}], \\ \nu_2 \partial_z q_2(0,t) = \nu_1 \partial_z q_1(0,t), & t \in [0,\mathcal{T}], \end{cases} \tag{3.1}$$

$$\begin{cases} \partial_t q_1 - \partial_z(\nu_1 \partial_z q_1) = f_1, & \text{in }]-L_1, 0[\times[0,\mathcal{T}], \\ q_1(-L_1, t) = 0, & t \in [0,\mathcal{T}], \\ q_1(0,t) = q_2(0,t), & t \in [0,\mathcal{T}]. \end{cases} \tag{3.2}$$

The complete setup for this simplified test-case is described in App. A, and a thorough mathematical and numerical study of this problem can be found in Lemarié et al. (2013b,c). We impose continuity of tracer q and its vertical flux at the interface. In Fig. 4 (left panel), we show the ℓ_2-norm of the errors associated with the synchronous and asynchronous methods. Based on purely numerical arguments, the synchronous method is preferable over the asynchronous one as it leads to a much reduced error. However, because the synchronous method does not satisfy the aforementioned physical constraints of the coupling and because the asynchronous method leads to significant numerical errors in the coupled solution, we strive to propose an alternative which theoretically provide a more consistent coupling.

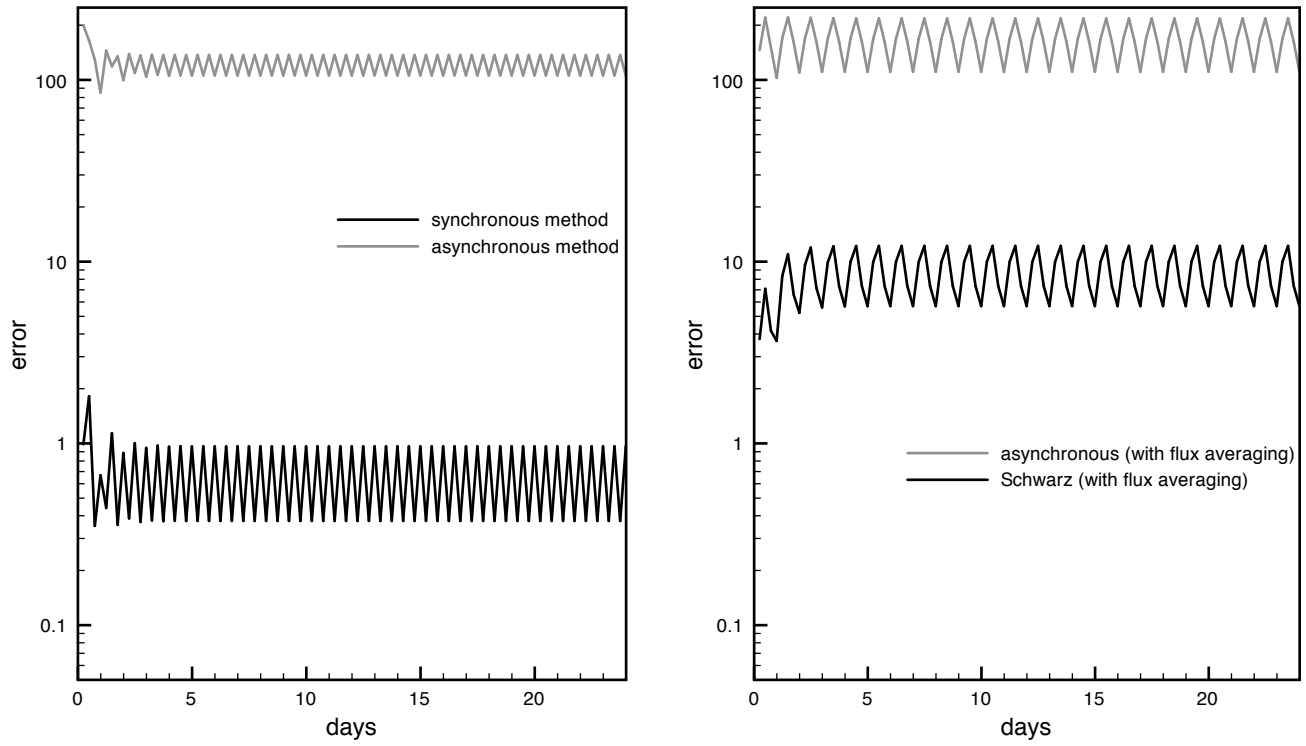

Fig. 4. Time history of the error ℓ_2-norm for different coupling methods : synchronous and asynchronous methods (left), asynchronous and global-in-time Schwarz methods with flux averaging (right).

3.3 Global in Time Schwarz Method

The Schwarz-like domain decomposition methods (see Gander, 2008, for a review) are widely used for coupling problems with different physics and/or different numerical treatment requirements. Originally introduced for stationary problems, those methods have been recently extended to time-dependent problems to provide a global-in-time Schwarz method, a.k.a. Schwarz waveform relaxation (e.g. Gander and Halpern, 2007). The idea is to separate the original problem on $\Omega = \Omega_{\rm atm} \cup \Omega_{\rm oce}$ into subproblems on $\Omega_{\rm atm}$ and $\Omega_{\rm oce}$, which can be solved separately. An iterative process is then applied to achieve the convergence to the solution of the original problem. The main drawback of this approach is the iterative procedure which increases the computational cost of the coupling, especially when the convergence is slow (note that there is currently an active work to develop methodologies aiming at optimizing the convergence speed of Schwarz-like methods, see discussion in Sec. 6). This kind of method has already been applied in an oceanic context with the goal of improving Poisson and Helmholtz solvers, open boundaries specification and nesting techniques (Debreu and Blayo, 1998; Blayo and Debreu, 2006; Cailleau et al., 2008) and seems well suited for our ocean-atmosphere coupling problem (1.4). Using the notations introduced previously, the iterative algorithm on a time window $[t_i, t_{i+1}]$ can be written as follows (for a given initial

condition at $t = t_i$) :

$$\text{Loop over } k \text{ until convergence}$$
$$\begin{cases} \mathcal{L}_{\rm atm}\mathbf{U}^{\rm a}_k = f_{\rm atm}, & \text{in } \Omega_{\rm atm} \times [t_i, t_{i+1}] \\ \mathcal{F}_{\rm atm}\mathbf{U}^{\rm a}_k = \mathbf{F}_{\rm oa}(\mathbf{U}^{\rm o}_{k-1}, \mathbf{U}^{\rm a}_k, \mathcal{R}_k), & \text{on } \Gamma \times [t_i, t_{i+1}] \\ \mathcal{L}_{\rm oce}\mathbf{U}^{\rm o}_k = f_{\rm oce}, & \text{in } \Omega_{\rm oce} \times [t_i, t_{i+1}] \\ \mathcal{F}_{\rm oce}\mathbf{U}^{\rm o}_k = \mathcal{F}_{\rm atm}\mathbf{U}^{\rm a}_k, & \text{on } \Gamma \times [t_i, t_{i+1}] \end{cases} \tag{3.3}$$

where the subscripts k denote the iteration number. The first guess $\mathbf{U}^{\rm o}_{k=0}$ on $\Gamma \times [t_i, t_{i+1}]$ is generally taken from the converged solution on the previous time window $[t_{i-1}, t_i]$. The two models, at each iteration, are run successively: this is the so called *multiplicative* form of the algorithm. If the condition $\mathcal{F}_{\rm oce}\mathbf{U}^{\rm o}_k = \mathcal{F}_{\rm atm}\mathbf{U}^{\rm a}_k$ is replaced by $\mathcal{F}_{\rm oce}\mathbf{U}^{\rm o}_k = \mathcal{F}_{\rm atm}\mathbf{U}^{\rm a}_{k-1}$ both models can be run in parallel over the whole time window $[t_i, t_{i+1}]$: this is the so called *parallel* form of the algorithm. When the convergence is reached, this algorithm gives the exact solution to (1.4). Note that with algorithm (3.3) the solution is independent of the length of the time windows $[t_i, t_{i+1}]$ which is not the case when performing only one iteration of this algorithm, as in the asynchronous coupling method. However, for the reasons mentioned above in Sec. 3.1, algorithm (3.3) should be modified to include a time-averaging procedure to the quantities near the air-sea interface as in (2.1):

$$\text{Loop over } k \text{ until convergence}$$
$$\begin{cases} \mathcal{L}_{\rm atm}\mathbf{U}^{\rm a}_k = f_{\rm atm}, & \text{in } \Omega_{\rm atm} \times [t_i, t_{i+1}] \\ \mathcal{F}_{\rm atm}\mathbf{U}^{\rm a}_k = \mathbf{F}_{\rm oa}\left(\left\langle \mathbf{U}^{\rm o}_{k-1} \right\rangle_i, \mathbf{U}^{\rm a}_k, \mathcal{R}_k\right), & \text{on } \Gamma \times [t_i, t_{i+1}] \\ \mathcal{L}_{\rm oce}\mathbf{U}^{\rm o}_k = f_{\rm oce}, & \text{in } \Omega_{\rm oce} \times [t_i, t_{i+1}] \\ \mathcal{F}_{\rm oce}\mathbf{U}^{\rm o}_k = \left\langle \mathcal{F}_{\rm atm}\mathbf{U}^{\rm a}_k \right\rangle_i, & \text{on } \Gamma \times [t_i, t_{i+1}] \end{cases} \tag{3.4}$$

In Fig. 4 (right panel), we show that the numerical errors using algorithm (3.4) are significantly reduced compared to the asynchronous method (2.1). Moreover, we numerically checked on a simple testcase that algorithm (3.4) converges.

3.4 Partial Conclusion

We have discussed so far the numerous delicacies we face when designing an AOCM. Those delicacies are both of numerical and physical nature. Before proceeding to a real-case study, we draw a few remarks based on our survey of the algorithmic aspects of ocean-atmosphere coupling. Looking at (2.1) and (3.4), it is clear that the asynchronous coupling method currently in use in global climate models corresponds to one iteration of the *multiplicative* form of a global-in-time Schwarz algorithm (Lemarié, 2008). In this respect, the asynchronous coupling is mathematically inconsistent because it does not give the solution of the coupling problem (1.4) but an approached one. Moreover, it can easily be shown that the synchronous coupling (2.2) is equivalent to one iteration of a local-in-time Schwarz algorithm (Cai and Sarkis, 1998). As described above, it is possible to satisfy the required consistency at the expense of an iterative process.

To avoid the burden of the iterations associated with Schwarz methods, a monolithic scheme (i.e. a

single model including both the oceanic and the atmospheric physics) may be used, but this method imposes the ocean and the atmosphere to be advanced on the same horizontal grid with the same time-step, which is unnatural in the case of space-time multi-physics problems. It must be clear that the Schwarz method is not expected to break any rule regarding the time-scale of physical processes. Convergence of the Schwarz method does not mean that we impose an instantaneous adjustment, e.g. of the oceanic boundary layer to the overlying atmospheric conditions. The objective is to ensure the proper regularity of the solution at the air-sea interface. In this respect, the iterative process associated with the Schwarz method should not be confused with the iterative methods sometimes used in convective adjustment schemes or Bulk formulations.

When using an iterative method, there are intertwined concerns : the computational cost and the convergence speed. The present paper is a preliminary study where attention is given to the impact of using Schwarz algorithm on the coupled solution, rather than its computational cost. However, it remains to verify first of all that the Schwarz method converges in the context of a practical application with realistic numerical models; we address this question numerically in the next section. To do so, we apply the *multiplicative Schwarz algorithm* to simulate the genesis and the propagation of cyclone Erica that occurred in March 2003 in the south-west Pacific ocean.

4 Model description and Experimental Setup

In this section we briefly present the numerical models we used to implement an AOCM as well as our coupling strategy based on algorithm (3.4).

4.1 Oceanic Model

The numerical oceanic model is ROMS (Shchepetkin and McWilliams, 2005) in its AGRIF-IRD [2] version, see Shchepetkin and McWilliams (2009) for a description of the various ROMS kernels. ROMS is a split-explicit time stepping, hydrostatic, Boussinesq, free-surface primitive equation model specifically designed for regional applications. ROMS equations are formulated using a generalized terrain-following σ-coordinate, that can be configured to enhance resolution in the surface boundary layer at the air-sea interface. Our experiment is setup in a configuration with four open boundaries, 50 σ-coordinate levels (grid parameters are chosen to ensure that the surface grid-box depth is at most 1 m), a horizontal grid with $\Delta x = 1/3^o$, and $\Delta t = 1800$s. The domain roughly extends from 6°S to 25°S in latitude and from 142.5°E to 172.5°E in longitude (Fig. 5). Note that a special care must be brought to the numerical schemes responsible for the tracer transport to properly simulate this area with complex bathymetry (Marchesiello et al., 2009). Vertical mixing of tracers and momentum to predict $\mathrm{K}_{\mathrm{m}}^{\mathrm{o}}(z)$ and $\mathrm{K}_{\mathrm{t}}^{\mathrm{o}}(z)$ is done with the KPP parameterization (Large et al., 1994). The coupled simulations are conducted without any flux correction scheme nor sea-surface temperature or salinity restoring. Model initialization results from a ten-year spin-up simulation forced by climatological atmospheric fluxes provided by the Comprehensive Ocean-Atmosphere Dataset (COADS) fields and by the QuikSCAT Climatology of Ocean Winds (QuikCOW). The oceanic boundary conditions are interpolated from a climatology based on the SODA reanalysis (the forcing fields are constructed using the Romstools utilities, Penven et al. (2008)). Note that the spin-up simulation develops large intrinsic variability at the mesoscale and is therefore uncorrelated at this scale with the actual motion (no data assimilation techniques were used).

4.2 Atmospheric Model

The atmospheric model used in our experiment is the WRF-ARW [3] solver (Skamarock and Klemp, 2008). WRF integrates the fully compressible nonhydrostatic Euler equations, those equations are formulated using a terrain-following mass vertical coordinate. The model grid has a horizontal resolution of $1/3°$ with 31 vertical levels and the time step is 180s. The meteorological data used for model initialization and boundary conditions are the NCEP2 reanalysis [4]. Note that there was no need for bogus injection to stimulate the cyclone generation in our simulations, as is sometimes done for cyclone studies, because the initial perturbation was captured by the NCEP2 reanalysis. The physical options used for the present study are the WSM3 (WRF Single-Moment 3-class) scheme for microphysics, the Rapid Radiative Transfer Model for longwave radiation, the Dudhia shortwave radiation scheme, the 5-layer thermal-diffusion land-surface model, and the Betts-Miller-Janjic cumulus parameterization. The Planetary Boundary Layer

[2] Adaptive Grid Refinement in Fortran-Institut de Recherche pour le Développement `http://roms.mpl.ird.fr/`

[3] Advanced Research WRF, `http://www.mmm.ucar.edu/wrf/users/`

[4] National Center for Environmental Prediction, `http://nomad3.ncep.noaa.gov/ncep_data/index.html`

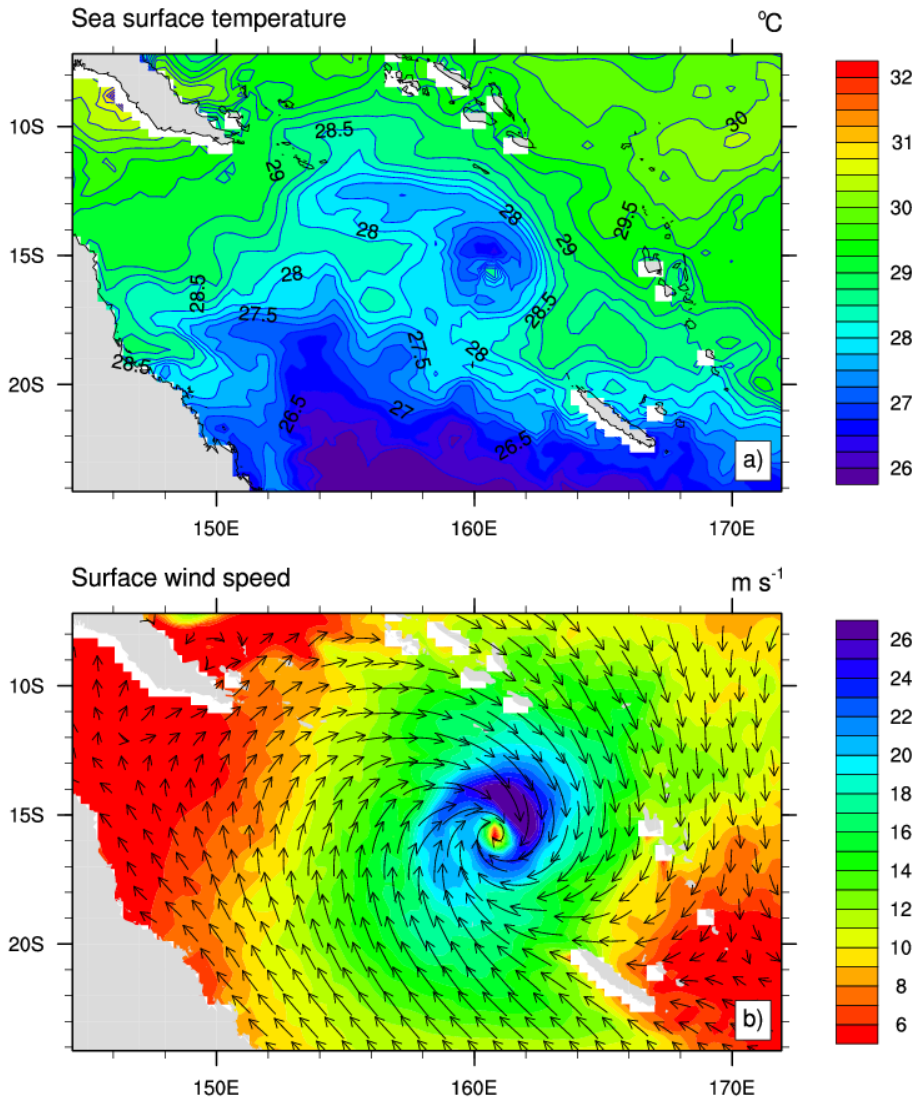

Fig. 5. Snapshots (March 12, 2003 at 8 p.m. GMT) of (a) ROMS sea surface temperature (b) WRF 10 meter winds during a coupled simulation.

scheme used to compute $\mathrm{K}^{\mathrm{a}}_{\mathrm{m}}(z)$ and $\mathrm{K}^{\mathrm{a}}_{\mathrm{t}}(z)$ is a non-local K-profile scheme (the Yonsei University (YSU) scheme, Hong et al. (2006)).

Similar WRF and ROMS configurations were used in an uncoupled mode in Jourdain et al. (2011) and Jullien et al. (2012) respectively to study the statistics of cyclonic activity over the South-Pacific, and the oceanic response to tropical cyclones.

4.3 Model Coupling Strategy

We implement a global-in-time Schwarz method to couple WRF and ROMS. In practice the different steps corresponding to algorithm (3.4) on a given time window $[t_i, t_{i+1}]$ and for iteration k are :

(1) Compute the atmospheric solution from t_i to t_{i+1} using $\mathbf{U}^{\mathrm{o}}_{k-1}$ (or $\mathbf{U}^{\mathrm{o}}_{[t_{i-1},t_i]}$ for $k=1$)
(2) Send averaged air-sea fluxes $\langle \mathcal{F}_{\mathrm{atm}} \mathbf{U}^{\mathrm{a}}_k \rangle_i$ on $[t_i, t_{i+1}]$ to the oceanic model
(3) Integrate the oceanic model on the same time period (knowing $\mathcal{F}_{\mathrm{atm}} \mathbf{U}^{\mathrm{a}}_k(t_i)$ and $\langle \mathcal{F}_{\mathrm{atm}} \mathbf{U}^{\mathrm{a}}_k \rangle_i$ fluxes are

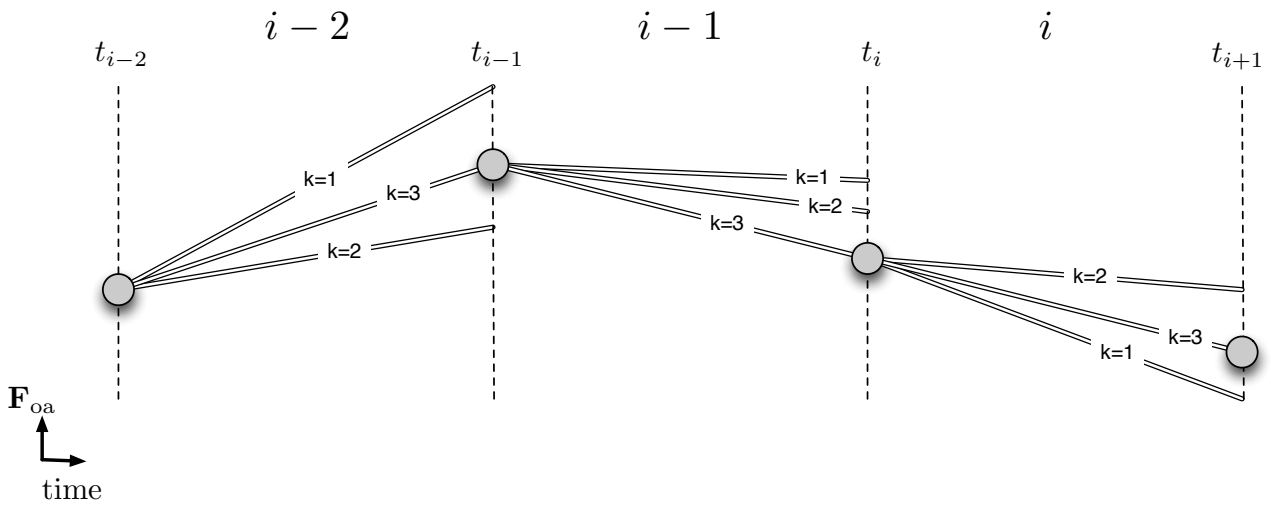

Fig. 6. Piecewise linear reconstruction of the air-sea fluxes for the oceanic model in the case of N = 3 iterations. The initial value (grey circles) and the average on a given time-window are sufficient to reconstruct the linear function.

linearly reconstructed, see Fig. 6)

(4) Send the newly computed $\mathbf{U}_k^{\mathrm{o}}$ to the atmospheric model.

Steps 1 to 4 are iteratively applied until convergence (or until a fixed number of iterations is attained). On each time-window $[t_i, t_{i+1}]$ the initial condition at $t = t_i$ corresponds to the converged solution from the previous time-window $[t_{i-1}, t_i]$. As mentioned earlier, one sequence of steps 1 to 4, without iterating, corresponds to (2.1).

In our practical implementation, the turbulent components of air-sea fluxes are computed in the WRF surface layer scheme based on a classical similarity theory which uses stability functions from Paulson (1970), Dyer and Hicks (1970), and Webb (1970) to compute the surface transfer coefficients for heat, moisture, and momentum. For our experiments we consider the same horizontal grids in WRF and ROMS. This is not a limitation of our method, this choice is done on purpose in order to ensure that we are only focusing on coupling errors and not interpolation/extrapolation errors.

4.4 Experimental Setup

The AOCM previously described is applied to simulate tropical cyclone Erica. Erica, a category 4 cyclone (on the Australia and Fiji scale), was generated in March 2003 off Australia and reached the New Caledonia region a few days later causing human and material damage. This event was poorly forecast, various simulations gave a totally different course than the real one. This kind of inaccuracies may occur when neglecting positive and negative feedbacks of the ocean to the atmosphere along the cyclone track. For instance, latent heat release to the atmosphere by the ocean is a positive feedback by which the ocean feeds cyclones. Representing the correct heat content of the upper ocean to which sea surface temperature (SST) is linked is thus of primary importance to simulate cyclogenesis.

The aim of the present preliminary study is to check the viability of the Schwarz method in a new context to address two important questions namely the convergence properties of the method in a fully realistic framework, and the impact of the coupling method on the coupled solution. Our analysis focuses on the inter-comparison between different coupling strategies and not on the direct comparison with observations of the real track (even if the track we get compares reasonably well with the real track, see Fig.

10). Indeed, the bulk formulations in WRF are not supposed to be designed for extreme situations and the effect of waves is neglected. This can be a source of significant discrepancies in data-model comparisons. Moreover, we can not expect an accurate simulation of maximum cyclone intensity because our horizontal grid spacing does not explicitely resolve small-scale vortices near the eyewall (Hill and Lackmann, 2009). Those vortices are responsible for an additional mixing and thus an alteration of the cyclone intensity. For all those reasons it is therefore more appropriate to consider here twin experiments conducted in an ensemblist way.

5 Numerical results

Let us now describe the framework designed to compare the various coupling methods introduced earlier. We restrict our comparison to the asynchronous (2.1) and the Schwarz (3.4) methods. As a matter of fact, the coupling methods at the time-step level are cumbersome and tedious to implement. Moreover, as explained earlier, the parameterizations we use are not adequate for this type of coupling.

5.1 Ensemble Design and Simulation Strategy

As mentioned in Sec. 1, AOCMs generally exhibit strong sensitivity to model parameters like the initial condition and/or the coupling frequency. To check whether this sensitivity is related to coupling errors, we design two ensembles of 18 members, each ensemble being integrated using a different coupling method. The 18 members are generated through perturbations of initial conditions and coupling frequency. We consider time windows of 3 hours and 6 hours, and three different initial conditions are chosen for the atmospheric and the oceanic models. The atmospheric model is started either from Feb. 28, or March 1 or March 2, corresponding to very distinct mesoscale situations (Fig. 7). As far as the oceanic model is concerned, we select from the 10 year climatological spin-up run three typical conditions for a month of March. Each coupled simulations are run till March 16, 2003. For the ensemble integrated using the Schwarz method we systematically proceed to $M = 9$ iterations. This is done to avoid choosing an arbitrary stopping criterion, and to keep the computational cost at a reasonable level.

5.2 Convergence Properties

First, it is natural to check the behavior of the coupled solution with respect to the iterations when the Schwarz method is used. To do so, we introduce a convergence rate R_k using the sea surface temperature $\overline{T}^{\mathrm{o}}(z=0)$ averaged in time on a given time window. R_k is defined as the ratio between the ℓ_2-norm of the error at two successive iterations, considering that the solution at iterate $k = M$ is the true solution of the problem :

$$R_k = \frac{\|e_k\|_2}{\|e_{k-1}\|_2} = \frac{\|\overline{T}^{\mathrm{o}}_k(z=0) - \overline{T}^{\mathrm{o}}_M(z=0)\|_2}{\|\overline{T}^{\mathrm{o}}_{k-1}(z=0) - \overline{T}^{\mathrm{o}}_M(z=0)\|_2}, \qquad \|e_k\|_2 = \sqrt{\sum_{i=1}^{n_x \times n_y} \left| \left(\overline{T}^{\mathrm{o}}_k\right)_i (z=0) - \left(\overline{T}^{\mathrm{o}}_M\right)_i (z=0) \right|^2}$$

with $\|\cdot\|_2$ the ℓ_2-norm, and n_x (resp. n_y) the number of grid points in the zonal (resp. meridional) direction. For the algorithm to converge R_k must remain smaller than unity, and the smaller R_k the faster the convergence. In this study, it turned out that four iterations were typically sufficient for convergence (Fig. 8). It is, however, expected that the convergence speed of the method should depend on the formulation of the AOCM in terms of physical parameterizations, as well as on the grid resolution. Finer resolution would lead to more energetic nonlinear effects which may impair the convergence speed of the method. These complications are left for a future study.

From a theoretical point of view, it is straightforward to show that the Schwarz Methods, and more generally iterative methods, are slower to converge in presence of low frequencies in the error. We can thus anticipate that the main differences in the coupled solutions integrated with a Schwarz method and an asynchronous method are mainly for low frequencies. In Fig. 9, the temporal spectrum

$$\mathrm{Sp}_\omega \left\{ \|\mathbf{u}^{\mathrm{a}}_h(z = 10\ \mathrm{m})_{k=M}\| - \|\mathbf{u}^{\mathrm{a}}_h(z = 10\ \mathrm{m})_{\mathrm{asyn}}\| \right\}$$

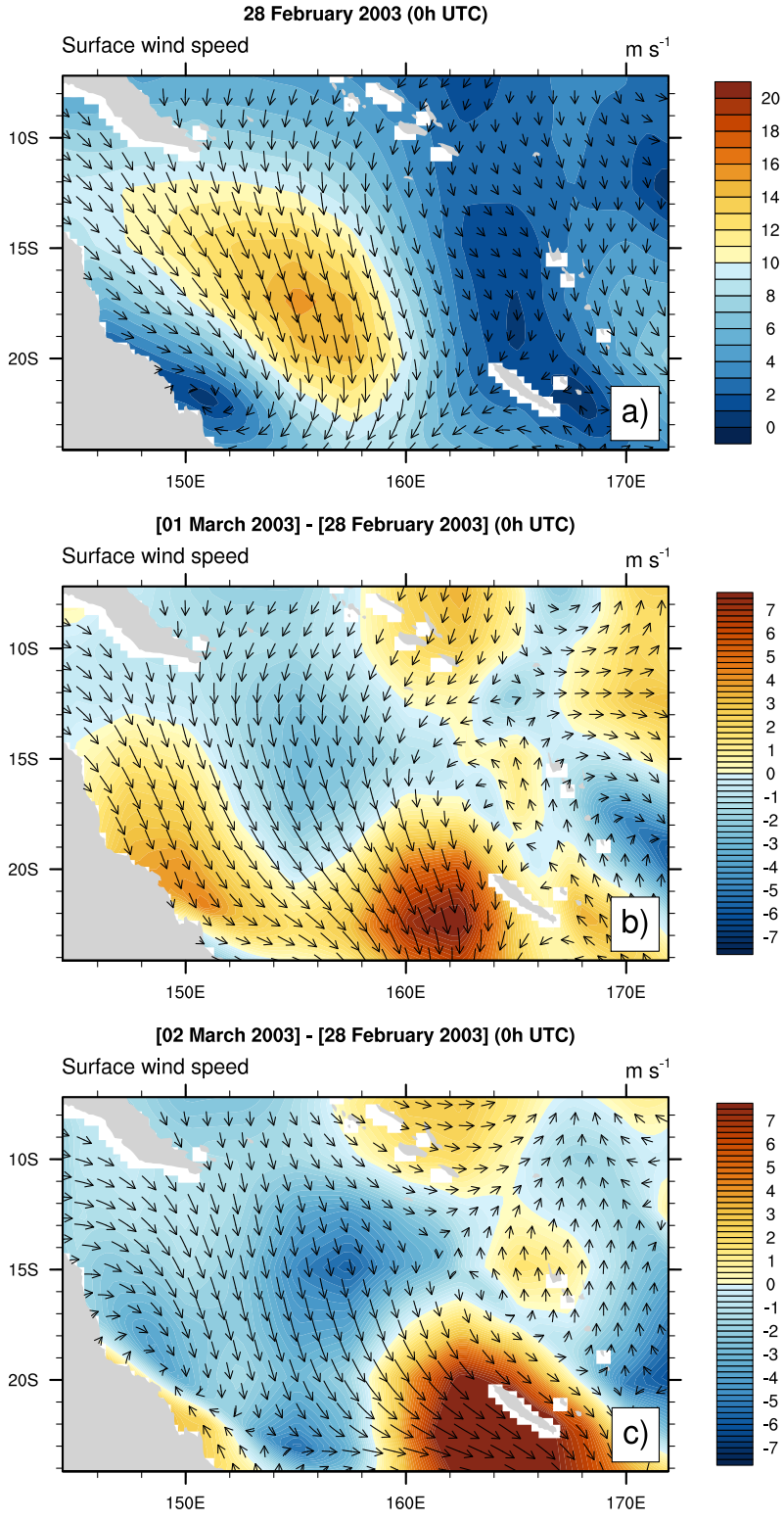

Fig. 7. Atmospheric surface winds initial condition for 28 Feb. 2003 (a), 01 Mar. 2003 (vectors, b), and 02 Mar. 2003 (vectors, c). Difference in wind speed between Mar. 01 and Feb. 28 (shaded, b), and between Mar. 02 and Feb. 28 (shaded, c)

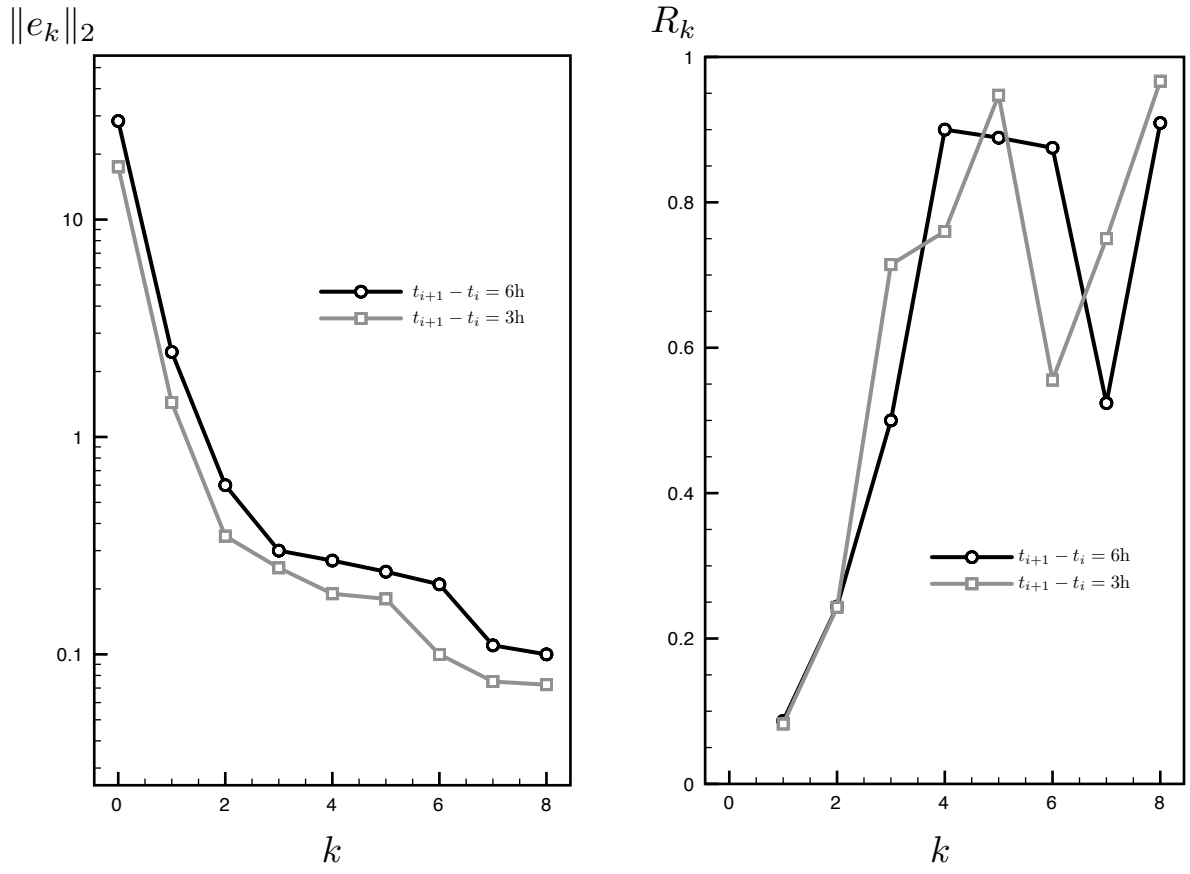

Fig. 8. Ensemble mean of the evolution of the error ℓ_2-norm (left) and of the convergence rate R_k with respect to the iterates k in the case of time windows of 3 hours and 6 hours.

of the difference between the asynchronous and the Schwarz methods is shown ($\mathbf{u}^{\mathrm{a}}_{h\,\mathrm{asyn}}$ being the solution obtained with the asynchronous method, i.e. one iteration only), with ω the frequency. The effect of the iterations is primarily visible for low time-frequencies which suggests that the Schwarz method may have a significant impact on long-term climate type studies. Note that it is theoretically possible to design a Schwarz method which could converge as quickly for all frequencies present in the error (this is the so-called *Optimized Schwarz Method*). However, this method is tractable only for relatively simple academic problems and is not straightforward to generalize to the ocean-atmosphere coupling problem (see discussion in Sec. 6).

5.3 Ensemble Spread

We checked so far that the Schwarz method converges in the particular case of our AOCM. Let us now illustrate the impact of the method on the robustness of the coupled solutions. Our comparison analysis of the various coupling methods will focus on the cyclone track and intensity for each member of the two ensembles. We define the track using the pressure minimum at the first vertical level of the atmospheric model. The various tracks shown in Fig. 11 approximately follow the real track with sea surface temperature and propagation speed in the same range (Fig. 10). It is striking to notice that the dispersion in the trajectories is significantly smaller for the ensemble integrated using the Schwarz method. In this case, the maximum standard deviation is 164 km and the standard deviation is around 92 km compared

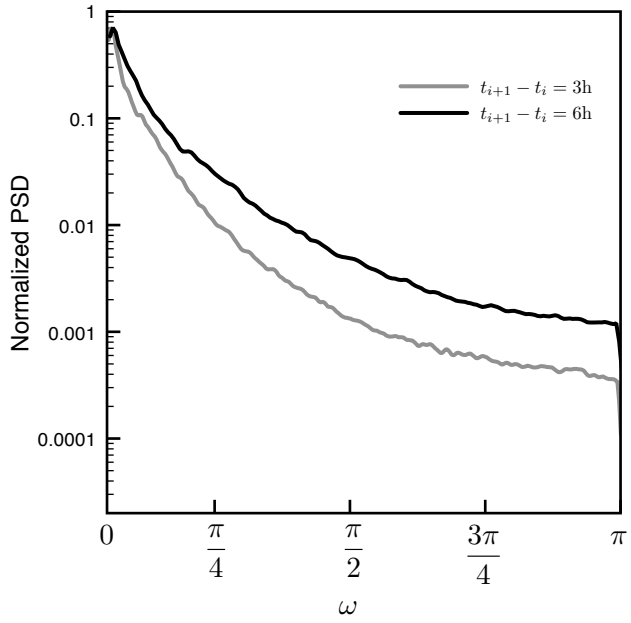

Fig. 9. Ensemble and spatial mean of the normalized power spectral density with respect to ω [h^{-1}] for difference in surface winds between the Schwarz and the asynchronous methods.

to respectively 212 km and 125 km with the asynchronous method. The same behavior can be seen in time histories of the maximum wind speed at 10 meters for each ensembles (not shown), with a maximum deviation of 6.2 m s^{-1} with the asynchronous method compared to 3.7 m s^{-1} with the Schwarz method (3.7 m s^{-1} versus 2.2 m s^{-1} for the standard deviation). The various tracks in the two ensembles tend to converge when approaching the south-east corner of the domain simply because each simulation has identical boundary conditions.

We showed that two very important features of cyclone events, namely the track and the intensity of the cyclone, are more robustly simulated when improving the consistency of the coupling method.

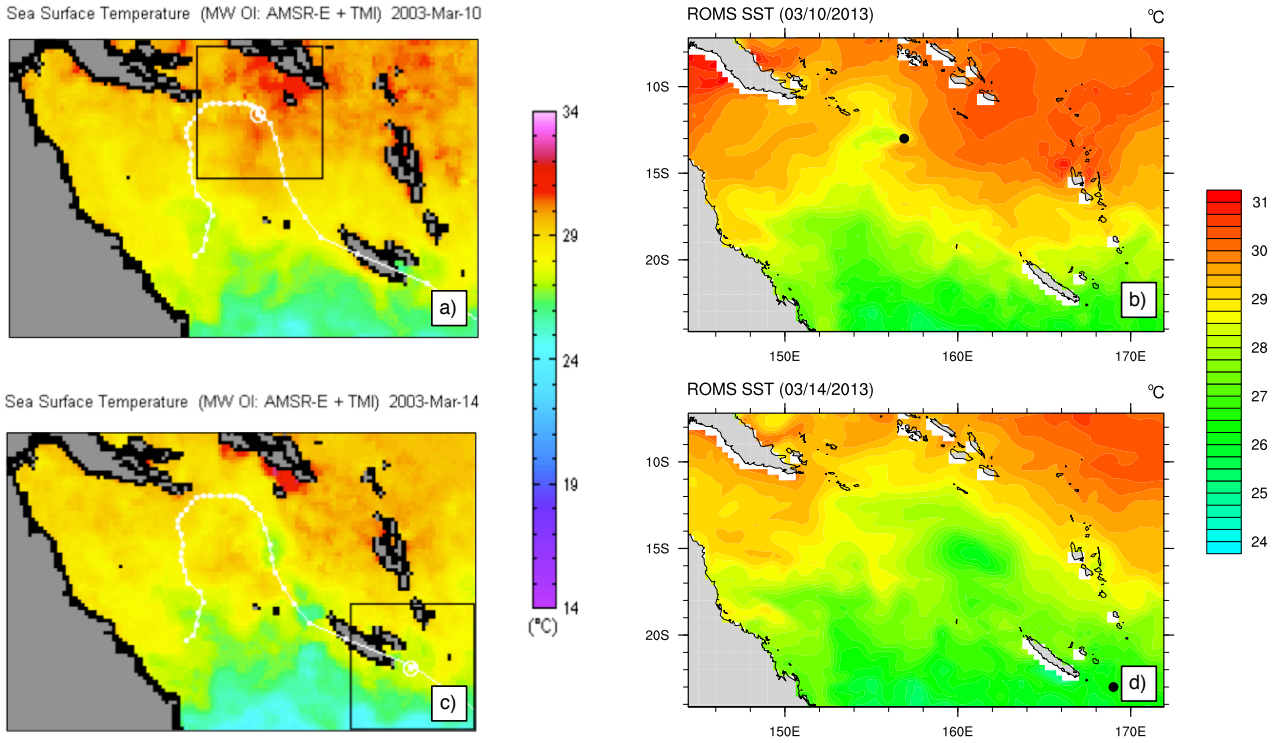

Fig. 10. Observed sea surface temperature [°C] (source : `http://www.ssmi.com/`) and cyclone track (white line) for March 10 (a) and March 14 (c). Same for a coupled solution (using the Schwarz method) (b and d). The black dots on b) and d) represent the location of the eye of the cyclone.

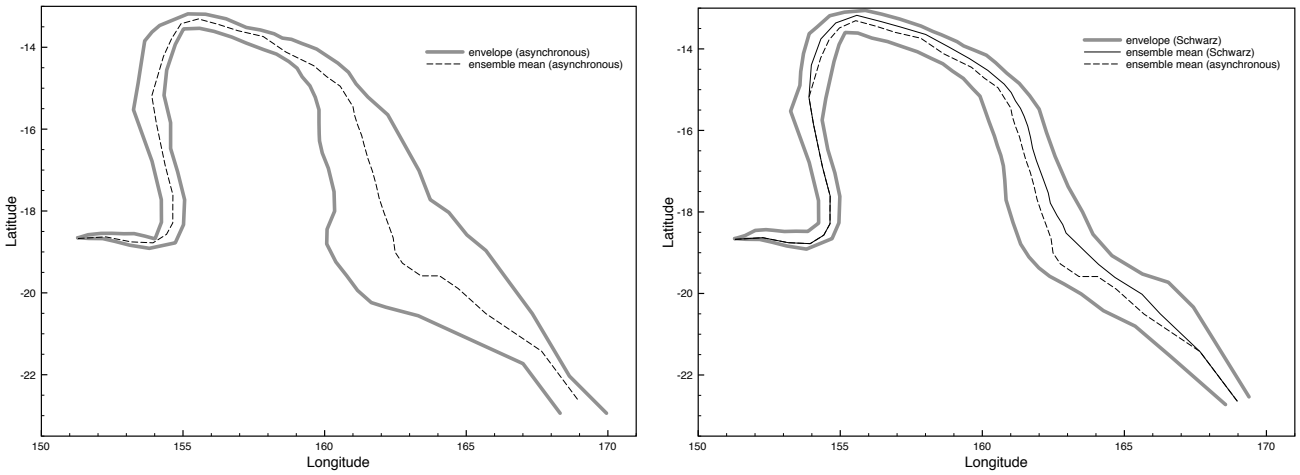

Fig. 11. Ensemble envelopes (thick gray lines) and means (thin black lines) for the cyclone track obtained with the asynchronous method (left) and Schwarz method (right) using the minimum pressure for the tracking.

6 Discussion and Conclusion

We have emphasized in this paper the key role of the coupling algorithm in the design of an Atmospheric and Oceanic Coupled Model (AOCM). We have seen that very popular coupling methods used in regional and global climate models do not provide the exact solution to the ocean-atmosphere coupling problem (1.4), but an approached one. We introduced a natural and little intrusive method to solve this problem and we showed its relevance. This method, called Global-in-Time Schwarz Method, is based on an iterative process which can substantially increase the computational cost of the AOCM (typically by a factor corresponding to the number of iterations to reach convergence). It can easily be shown that the usual synchronous (2.2) and asynchronous (2.1) methods in vogue in climate models correspond to only one iteration of a Schwarz algorithm.

Numerical results conducted in an ensemblist way through perturbations of the initial conditions and coupling frequency of a realistic regional AOCM suggest that part of the sensitivity to those parameters can be attributed to inaccuracies in the coupling method. Moreover, for our particular case, it seems that three iterations of the Schwarz method are sufficient to improve the coupled solutions with respect to their sensitivity to model parameters. We showed that the iterative process is expected to significantly modify the low-frequency component of the solution, whereas the high-frequencies converge very rapidly. We might anticipate that the effect of the iterations could be even more acute for long-term climate type studies. However, it remains to be checked that the iterative process converges whatever the formulation of the AOCM, and more particularly whatever the boundary layer parameterizations at the air-sea interface. We can speculate that the Schwarz algorithm can bring theoretical tools useful to assess a measure of "compatibility" between atmospheric and oceanic boundary layer parameterizations : two schemes could be recognized as *compatible* as long as they lead to a converging Schwarz algorithm.

Under some circumstances, the computational cost of the Schwarz algorithm may not be affordable for all type of applications and one can proceed to only one iteration of the method, thus retrieving the asynchronous method. Based on our study and on our earlier work at a theoretical level (Lemarié et al., 2013a,b,c), we can formulate some recommendations when the asynchronous coupling method is used :

- The coupling frequency (i.e. the size of the time windows between two exchanges of boundary conditions between the models) can be adequately set to minimize the coupling errors and the error of parameterization of the surface fluxes. Because the Schwarz algorithm converges slowly for the low-frequencies in the error, the shorter the time window the smaller the coupling error. Because of the large uncertainties in the specification of the surface fluxes, the larger the time window the smaller the parameterization error. Taking those constraints into account and the requirement of a proper representation of the diurnal cycle, a coupling frequency between 1 and 3 hours is expected to provide a good compromise between the various sources of errors at play. Moreover, it is generally observed that the wave field acts as a low-pass filter on the air-sea exchange, with a cutoff around 2 hours, which suggests that time windows of 2 hours could be considered as a relevant value for AOCMs.
- In Lemarié et al. (2013b,c), it is shown that the type of interface condition has great impact on the convergence speed of the Schwarz algorithm. In the case of a diffusion problem, replacing Dirichlet-Neumann [5] conditions by Robin (a.k.a. Fourier) interface condition (i.e. a linear combination of a Dirichlet and a Neumann condition) can dramatically improve the convergence speed if the weights in the linear combination are properly chosen. It can be shown that even in the case of one single itera-

[5] A Dirichlet condition amounts to specifying a value in the interface, whereas a Neumann condition amounts to specifying a flux.

tion of the method (i.e.; the asynchronous method) the coupling errors can be reduced just by working on the type of interface conditions. However, in the context of AOCMs, this is not an easy task to do because we have to deal with the Bulk formulation in the theoretical study. This is a work in progress.

Acknowledgements

F. Lemarié and E. Blayo acknowledge the support of the French LEFE-MANU (Les Enveloppes Fluides et l'Environnement, méthodes MAthématiques et NUmériques) program through project COCOA (COuplage Côtes, Océan, Atmosphère). L. Debreu and P. Marchesiello were funded by the ANR through contract ANR-11-MONU-005 (COMODO). Authors are grateful to Gurvan Madec for helpful discussions and suggestions.

References

Bao, J.W., Wilczak, J.M., Choi, J.K., Kantha, L.H., 2000. Numerical simulations of air-sea interaction under high wind conditions using a coupled model : A study of hurricane development. Mon. Weather Rev. 128(7), 2190–2210.

Bengtsson, L., 1999. From short-range barotropic modelling to extended-range global weather prediction: a 40-year perspective. Tellus B 51(1), 13–32.

Blayo, E., Debreu, L., 2006. Nesting ocean models, in: Chassignet, E., Verron, J. (Eds.), An Integrated View of Oceanography: Ocean Weather Forecasting in the 21st Century. Kluwer.

Bryan, F., Kauffman, B., Large, W., Gent, P., 1996. The ncar csm flux coupler. Technical Report NCAR/TN-424+STR. NCAR.

Cai, X.C., Sarkis, M., 1998. Local multiplicative schwarz algorithms for steady and unsteady convection-diffusion equations. East-West J. Numer. Math. 6, 27–41.

Cailleau, S., Fedorenko, V., Barnier, B., Blayo, E., Debreu, L., 2008. Comparison of different numerical methods used to handle the open boundary of a regional ocean circulation model of the bay of biscay. Ocean Modell. 25(1-2), 1–16.

Capet, X., Colas, F., McWilliams, J.C., Penven, P., Marchesiello, P., 2008. Eddies in eastern-boundary subtropical upwelling systems, in: Hecht, M., Hasumi, H. (Eds.), Ocean Modeling in an Eddying Regime. American Geophysical Union, USA. volume 177 of *Geophysical Monograph Series*, p. 350.

Colas, F., McWilliams, J.C., Capet, X., Kurian, J., 2011. Heat balance and eddies in the Peru-Chile Current System. Clim. Dynam. In press.

Danabasoglu, G., Large, W.G., Tribbia, J.J., Gent, P.R., Briegleb, B.P., McWilliams, J.C., 2006. Diurnal coupling in the tropical oceans of ccsm3. J. Climate 19(11), 2347–2365.

Debreu, L., Blayo, E., 1998. On the schwarz alternating method for oceanic models on parallel computers. J. Comp. Phys. 141(2), 93 – 111.

Dyer, A.J., Hicks, B.B., 1970. Flux-gradient relationships in the constant flux layer. Quart. J. Roy. Meteorol. Soc. 96(410), 715–721.

Fairall, C.W., Bradley, E.F., Hare, J.E., Grachev, A.A., Edson, J.B., 2003. Bulk parameterization of air-sea fluxes: updates and verification for the COARE algorithm. J. Climate 16, 571–591.

Gander, M.J., 2008. Schwarz methods over the course of time. Electron. Trans. Numer. Anal. 31, 228–255.

Gander, M.J., Halpern, L., 2007. Optimized Schwarz waveform relaxation methods for advection reaction diffusion problems. SIAM J. Numer. Anal. 45(2), 666–697 (electronic).

Hill, C., DeLuca, C., Balaji, V., Suarez, M., Silva, A.d., 2004. The Architecture of the Earth System Modeling Framework. Computing in Science and Engg. 6, 18–28.

Hill, K.A., Lackmann, G.M., 2009. Analysis of idealized tropical cyclone simulations using the weather research and forecasting model: Sensitivity to turbulence parameterization and grid spacing. Mon. Weather Rev. 137(2), 745765.

Hong, S.Y., Noh, Y., Dudhia, J., 2006. A new vertical diffusion package with an explicit treatment of entrainment processes. Mon. Weather Rev. 134, 2318–2341.

Joppich, W., Kürschner, M., 2006. MpCCI - a tool for the simulation of coupled applications. Concurr. Comput. : Pract. Exper. 18, 183–192.

Jourdain, N.C., Marchesiello, P., Lefèvre, C.E., Vincent, E., Lengaigne, M., Chauvin, F., 2011. Mesoscale simulation of tropical cyclones in the south pacific : climatology and interannual variability. J. Climate 24, 3–25.

Jullien, S., Menkès, C., Marchesiello, P., Jourdain, N.C., Lengaigne, M., Koch Larrouy, A., Lefevre, J., Vincent, E.M., Faure, V., 2012. Impact of tropical cyclones on the heat budget of the South Pacific Ocean. J. Phys. Oceanogr. 42, 1882–1906.

Large, W.G., 2006. Surface fluxes for practitioners of global ocean data assimilation, in: Chassignet, E., Verron, J. (Eds.), An Integrated View of Oceanography: Ocean Weather Forecasting in the 21st Century. Kluwer.

Large, W.G., Danabasoglu, B., 2006. Attribution and impacts of upper-ocean biases in CCSM3. J. Climate 19(11), 2325–2346.

Large, W.G., McWilliams, J.C., Doney, S.C., 1994. Oceanic vertical mixing: A review and a model with a nonlocal boundary layer parameterization. Rev. Geophys. 32(4), 363–403.

Lebeaupin Brossier, C., Ducrocq, V., Giordani, H., 2008. Sensitivity of three mediterranean heavy rain events to two different sea surface fluxes parameterizations in high-resolution numerical modeling. J. Geophys. Res. 113.

Lebeaupin Brossier, C., Ducrocq, V., Giordani, H., 2009. Effects of the air-sea coupling time frequency on the ocean response during mediterranean intense events. Ocean Dyn. 59, 539–549.

Lemarié, F., 2008. Algorithmes de Schwarz et couplage océan-atmosphère. Thesis (Ph.D.)–Grenoble University (France).

Lemarié, F., Debreu, L., Blayo, E., 2013a. Optimal control of the convergence rate of schwarz waveform relaxation algorithms. Lecture Notes in Computational Science and Engineering 91, 599–606.

Lemarié, F., Debreu, L., Blayo, E., 2013b. Toward an optimized global-in-time schwarz algorithm for diffusion equations with discontinuous and spatially variable coefficients, part 1 : the constant coefficients case. Electron. Trans. Numer. Anal. 40, 148–169.

Lemarié, F., Debreu, L., Blayo, E., 2013c. Toward an optimized global-in-time schwarz algorithm for diffusion equations with discontinuous and spatially variable coefficients, part 2 : the variable coefficients case. Electron. Trans. Numer. Anal. 40, 170–186.

Lemarié, F., Kurian, J., Shchepetkin, A.F., Molemaker, M.J., Colas, F., McWilliams, J.C., 2012. Are There Inescapable Issues Prohibiting the use of Terrain-Following Coordinates in Climate Models ? Ocean Modell. 42, 57–79.

Lions, J.L., Temam, R., Wang, S., 1995. Mathematical theory for the coupled atmosphere-ocean models. J. Math. Pures Appl. 74, 105–163.

Marchesiello, P., Debreu, L., Couvelard, X., 2009. Spurious diapycnal mixing in terrain-following coordinate models: The problem and a solution. Ocean Modell. 26(3-4), 159–169.

Marchesiello, P., McWilliams, J.C., Shchepetkin, A.F., 2003. Equilibrium structure and dynamics of the

California Current System. J. Phys. Oceanogr. 33(4), 753–783.
Masson, S., Terray, P., Madec, G., Luo, J.J., Yamagata, T., Takahashi, K., 2012. Impact of intra-daily SST variability on ENSO characteristics in a coupled model. Clim. Dynam. 39(3-4), 681–707.
McWilliams, J.C., 2007. Irreducible imprecision in atmospheric and oceanic simulations. Proc. Natl. Acad. Sci. 104(21), 8709–8713. http://www.pnas.org/content/104/21/8709.full.pdf+html.
Muller, H., Dumas, F., Blanke, B., Mariette, V., 2007. High-resolution atmospheric forcing for regional oceanic model: the iroise sea. Ocean Dyn. 57, 375–400.
Paulson, C.A., 1970. The mathematical representation of wind speed and temperature profiles in the unstable atmospheric surface layer. J. Appl. Meteorol. 9(6), 857–861.
Penven, P., Marchesiello, P., Debreu, L., Lefèvre, J., 2008. Software tools for pre- and post-processing of oceanic regional simulations. Environ. Mod. Software 23(5), 660–662.
Perlin, N., Skyllingstad, E.D., Samelson, R.M., Barbour, P.L., 2007. Numerical simulation of air-sea coupling during coastal upwelling. J. Phys. Oceanogr. 37(8), 2081–2093.
Ploshay, J., Anderson, J., 2002. Large sensitivity to initial conditions in seasonal predictions with a coupled ocean-atmosphere general circulation model. J. Geophys. Res. 29.
Redler, R., Valcke, S., Ritzdorf, H., 2010. OASIS4 - a coupling software for next generation earth system modelling. Geoscientific Model Development 3(1), 87–104.
Roehrig, R., Bouniol, D., Guichard, F., Hourdin, F., Redelsperger, J.L., 2013. The present and future of the west african monsoon: a process-oriented assessment of cmip5 simulations along the amma transect. J. Climate Doi: http://dx.doi.org/10.1175/JCLI-D-12-00505.1.
Sen Gupta, A., Jourdain, N.C., Brown, J.N., D., M., 2013. Climate drifts in the cmip5 models. J. Climate In press.
Shchepetkin, A., McWilliams, J.C., 2005. The Regional Oceanic Modeling System (ROMS): A split-explicit, free-surface, topography-following-coordinate ocean model. Ocean Modell. 9(4), 347–404.
Shchepetkin, A., McWilliams, J.C., 2009. Correction and commentary for "Ocean forecasting in terrain-following coordinates: Formulation and skill assessment of the Regional Ocean Modelling System" by Haidvogel et al., J. Comp. Phys. 227, pp. 3595-3624. J. Comp. Phys. 228(24), 8985–9000.
Skamarock, W.C., Klemp, J.B., 2008. A time-split nonhydrostatic atmospheric model for weather research and forecasting applications. J. Comp. Phys. 227, 3465–3485.
Terray, P., Masson, S., Kakitha, K., Sahai, A.K., Luo, J.J., 2011. The role of the frequency of SST coupling in the Indian Monsoon variability and monsoon-ENSO-IOD relationships in a global coupled model. Clim. Dynam. 39(3-4), 729–754.
Tribbia, J.J., Baumhefner, D.P., 1988. The reliability of improvements in deterministic short-range forecasts in the presence of initial state and modeling deficiencies. Mon. Weather Rev. 116, 2276–2288.
Webb, E.K., 1970. Profile relationships: The log-linear range, and extension to strong stability. Quart. J. Roy. Meteorol. Soc. 96(407), 67–90.

A Test Problem: One-Dimensional Diffusion Problem

In this section, we aim at comparing different coupling methods using a simple testcase meant to be representative of an ocean-atmosphere type problem. To do so, we define two subdomains $\Omega_1 =]-L_1, 0[$ and $\Omega_2 =]0, L_2[$ with $L_1 = L_2 = 250$ m. In this example, we consider the one dimensional diffusion equation of a scalar quantity q

$$\partial_t q - \partial_z \left(\nu \partial_z q\right) = f, \tag{A.1}$$

with ν a diffusion coefficient such that $\nu = \nu_1$ in Ω_1 and $\nu = \nu_2$ in Ω_2. We choose $\nu_1 \neq \nu_2$ to model the heterogeneous physical properties between the two subdomains. Uniqueness of solutions for the coupling problem is obtained with Dirichlet-Neumann conditions at $z = 0$ (i.e. we require the equality of the subproblems solutions and of their fluxes). The corresponding coupling problem reads

$$\begin{cases} \partial_t q_2 - \partial_z(\nu_2 \partial_z q_2) = f_2, & \text{in }]0, L_2[\times[0, \mathcal{T}], \\ q_2(L_2, t) = \widetilde{q}_2(t), & t \in [0, \mathcal{T}], \\ \nu_2 \partial_z q_2(0, t) = \nu_1 \partial_z q_1(0, t), & t \in [0, \mathcal{T}], \end{cases} \tag{A.2}$$

$$\begin{cases} \partial_t q_1 - \partial_z(\nu_1 \partial_z q_1) = f_1, & \text{in }]-L_1, 0[\times[0, \mathcal{T}], \\ q_1(-L_1, t) = \widetilde{q}_1(t), & t \in [0, \mathcal{T}], \\ q_1(0, t) = q_2(0, t), & t \in [0, \mathcal{T}], \end{cases} \tag{A.3}$$

for a given initial condition. We pose the problem to get analytical solutions of the form

$$q_2(z,t) = \frac{q_0}{8}\left[3 - \exp\left(-\frac{z}{\alpha_2}\right)\right]\left[1 + \cos^2\left(\frac{\pi t}{T}\right)\right]$$

$$q_1(z,t) = \frac{q_0}{8}\left[1 + \exp\left(\frac{z}{\alpha_1}\right)\right]\left[1 + \cos^2\left(\frac{\pi t}{T}\right)\right]$$

where the condition $\nu_2\alpha_1 = \nu_1\alpha_2$ is sufficient to ensure the proper regularity of the solution across the interface at $z = 0$. To obtain such analytical solutions, we set the right hand sides f_1 and f_2

$$f_1(z,t) = -\frac{q_0}{8}\left\{\left(\frac{\pi}{T}\sin\frac{2\pi t}{T}\right)\left[1 + \exp\left(\frac{z}{\alpha_1}\right)\right] + \frac{\nu_1}{\alpha_1^2}\exp\left(\frac{z}{\alpha_1}\right)\left[1 + \cos^2\left(\frac{\pi t}{T}\right)\right]\right\},$$

$$f_2(z,t) = -\frac{q_0}{8}\left\{\left(\frac{\pi}{T}\sin\frac{2\pi t}{T}\right)\left[3 - \exp\left(-\frac{z}{\alpha_2}\right)\right] - \frac{\nu_2}{\alpha_2^2}\exp\left(-\frac{z}{\alpha_2}\right)\left[1 + \cos^2\left(\frac{\pi t}{T}\right)\right]\right\}.$$

Equation (A.1) is discretized using a backward Euler scheme in time and a second-order scheme on a staggered grid in space. The parameter values are $\alpha_1 = 50$, $\alpha_2 = 10$, $q_0 = 15$, $T_0 = 24 \times 3600$ s, $\nu_1 = 1$ m s^{-1}, $\nu_2 = 0.2$ m s^{-1}, $\Delta z = 1$ m, $\Delta t = 900$ s, and the total simulation time is $\mathcal{T} = 2000$ days. To numerically solve the coupling problem (A.2-A.3), we use the six different methods described in the paper : the asynchronous method with instantaneous and averaged fluxes (the fluxes are reconstructed using a linear conservative scheme), the global-in-time Schwarz method with instantaneous and averaged fluxes, the synchonous method and the local-in-time Schwarz method. The global-in-time Schwarz method and the asynchronous method are integrated with time windows of 6 hours. As expected, the Schwarz methods (local or global in time) with instantaneous fluxes provide strictly the same solution $q^\star(z,t)(z \in \Omega_1 \bigcup \Omega_2, t \in [0, \mathcal{T}])$ which is used as a reference to compute the ℓ_2-norm of the error for other methods

$$\|\varepsilon(t_i)\|_2 = \sqrt{\sum_{k=1}^{k=N} |q(z_k, t_i) - q^\star(z_k, t_i)|^2},$$

with N the number of grid points between $-L_1$ and L_2. The time evolution of $\|\varepsilon\|_2$ is represented in Fig. 4, and discussed in Sec. 3.2 and 3.3.